JOURNAL OF MATERIALS SCIENCE **39** (2004) 3733–3737

Fracture behavior of ultra-fine grained steel bar under dynamic loading

H. QIU, Y. KAWAGUCHI
Steel Research Center, National Institute for Material Science, 1-2-1 Sengen, Tsukuba, Ibaraki 305-0047, Japan
E-mail: qiu.hai@nims.go.jp

C. SHIGA
VUZ Welding Research Institute, Racianska 71, Bratislava 832 59, Slovakia

Ultra-fine grained steel bars were recently developed by thermo-mechanical controlled rolling with rapid cooling for increasing the strength of low carbon and low alloy steels. The developed steels are characterized by fine ferrite grains of less than 1 μm and high strength as a result of grain refinement. However, their correlations between tensile properties and impact behavior are not well understood. In this paper, impact absorbed energy (E_p) and dynamic fracture toughness (J_{Id}) were used to evaluate the dynamic fracture behavior of the ultra-fine grained steels, and the fracture mechanisms were also investigated. For the ultra-fine grained steels, tensile stress-strain curve was shown to be correlated with the impact curve of load vs. time, and to be related to the dynamic fracture toughness. The steel with large ferrite grains, small ferrite grain colony and martensite was found to have a good combination of strength and toughness. © *2004 Kluwer Academic Publishers*

1. Introduction

The strength of steels is generally increased by adding suitable alloying elements or refining grain size. Addition of alloying elements is effective to increase the tensile strength, however, toughness and ductility are decreased significantly. Grain refinement has been shown to be effective to increase both strength and toughness. Ferrite grains in steels can be only reduced to ~5 μm in diameter by general thermo-mechanical controlled processing (TMCP) [1]. Recently, ultra-fine grained steel bars with ferrite grains of less than 1 μm were successfully developed [2–4].

The developed low carbon ultra-fine grained steel bars have been shown to have high strength (800 MPa) [5], however, the fracture behavior under dynamic loading was not well understood. In this paper, the impact behavior of the ultra-fine grained steels was evaluated in terms of dynamic fracture toughness and absorbed energy, which were measured on an instrumented Charpy test machine. The fracture mechanisms caused by impact loading were investigated by a scanning electron microscope. The correlation of the impact curve with the tensile stress strain curve was also discussed. The experimental results obtained on the specimens of appropriate microstructure show a good impact behavior combined with high strength.

2. Experimental details

2.1. Fabrication of ultra-fine grained steel bars

Two chemical composition series (A and B) were selected as shown in Table I. Except for Nb and Ti, the other compositions of series A and B are almost the same, and are similar to those of the mild steel. Low values of P_{cm} (welding crack sensitivity) indicate that series A and B have superior weldability against cold cracking. The ingots with chemical composition series A and B were processed from two directions (X and Y) by a grooved rolling-machine shown in Fig. 1. The rolling procedures are shown in Fig. 2. For series A, an ingot of 115 mm in diameter was kept at 1200°C in the furnace for 1 h to get uniform austenite, and then the ingot was taken out and cooled down to 750°C in air. At 750°C, the ingot was rolled 27 passes. After the 27 passes, the ingot was rolled into a bar with a

TABLE I Chemical composition (mass%)

No.	*C*	Si	Mn	*P*	*S*	Al	*N*	Nb	Ti	P_{cm}(%)[a]
A	0.09	0.30	1.45	0.010	0.0008	0.029	0.0012	0.018	0.006	0.173
B	0.09	0.30	1.44	0.009	0.0008	0.029	0.0012	–	–	0.172

[a] $P_{cm}(\%) = C + Si/30 + Mn/20 + Cu/20 + Ni/60 + Cr/20 + Mo/15 + V/10 + 5B$.

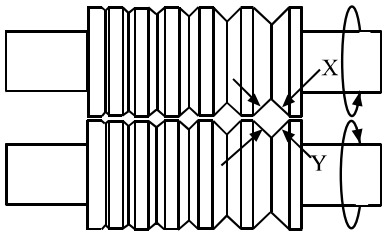

Figure 1 Schematic illustration of grooved rolling machine.

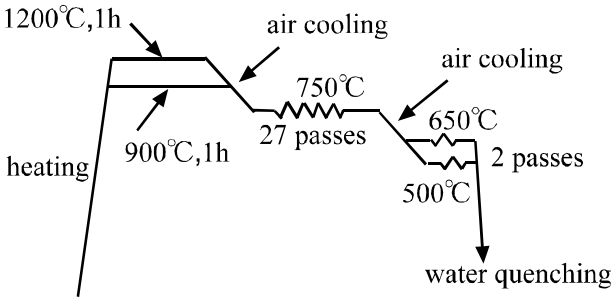

Figure 2 Schematic illustration of rolling processes.

square cross section of 24 mm × 24 mm. At 750°C, the steel bar was cut into two parts. One part of the steel bar was cooled down to 650°C in air, and the other down to 500°C. They were again rolled 2 passes at 650 and 500°C, respectively and then were immediately water-quenched. The final size of the cross-section of the square bars is ∼18 mm × 18 mm. An ingot of series B was initially kept at 900°C instead of 1200°C for 1 h, and the following process procedures were exactly the same as series A. In this paper, the steel bars finally rolled at 650 and 500°C are denoted as A1 and A2, respectively, for series A, and B1 and B2, respectively, for series B.

2.2. Experimental method

Tensile specimens with a diameter of 8 mm and a gage length of 40 mm and fatigue pre-cracked three-point bending specimens (10 mm × 10 mm × 55 mm) with a pre-crack length of ∼2 mm prepared from the 18 mm × 18 mm square bars were applied for tensile and impact tests. Tensile tests were conducted at room temperature with a crosshead speed of 0.4 mm per min. Impact tests were carried out on an instrumented Charpy test machine. The dynamic fracture toughness of A1, A2, B1 and B2 was evaluated by J_{Id}, which was given by

$$J_{Id} = \frac{2A_p}{B(W-a)} \tag{1}$$

where A_p is the area from zero to the maximum load in the load vs. displacement impact curve, B is the width, W is the height, and a is the fatigue pre-crack length.

The microstructures were observed under optical microscopy and Scanning Electron Microscopy (SEM), and the fracture surfaces of tensile and impact specimens were examined by SEM.

3. Results and discussion

3.1. Microstructure

The SEM microstructures of A1, A2, B1 and B2 vertical to the rolling direction are shown in Fig. 3. Both

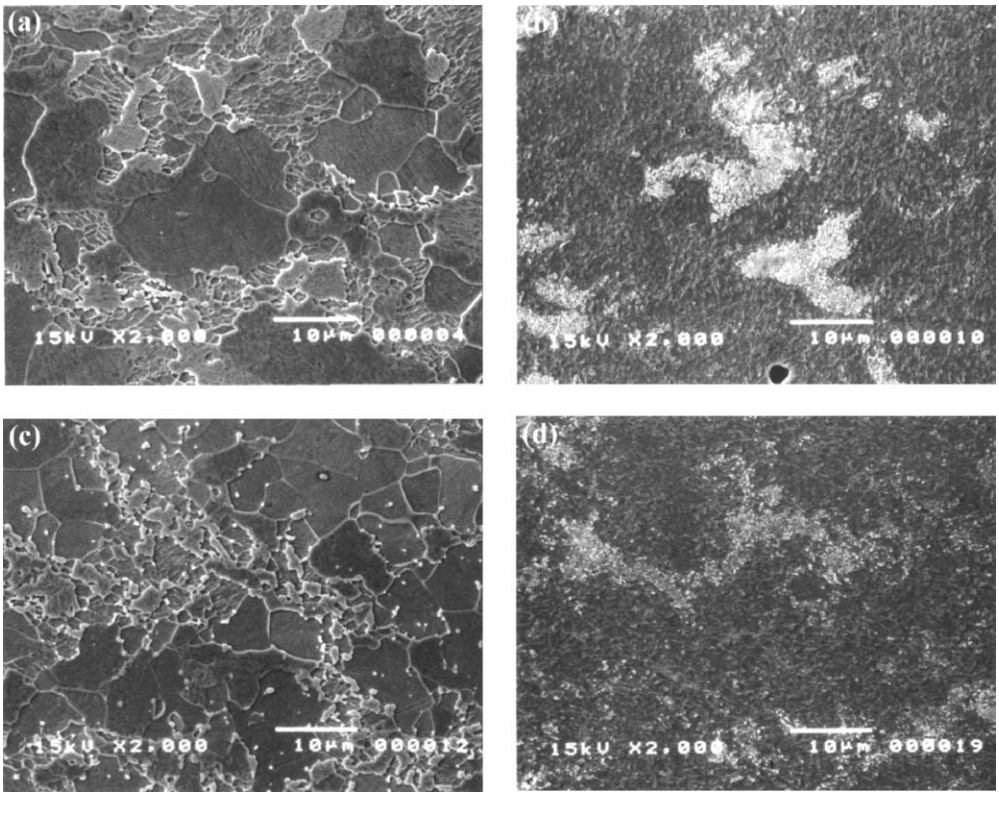

Figure 3 SEM micrographs of (a) A1, (b) A2, (c) B1 and (d) B2 vertical to the rolling direction.

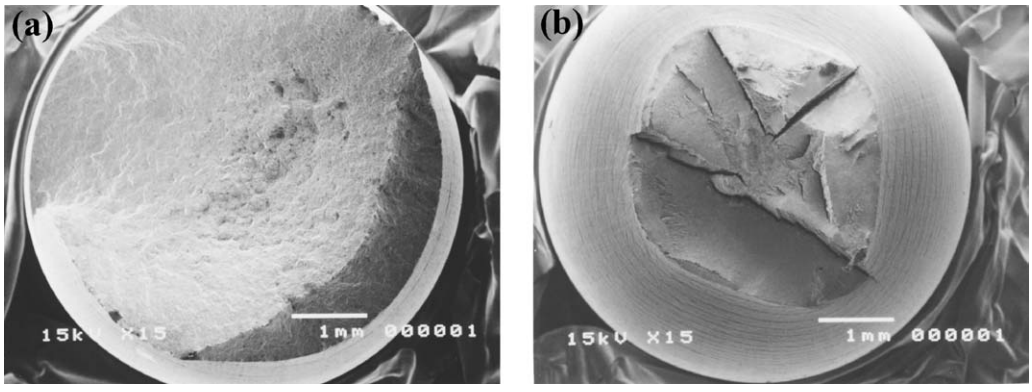

Figure 4 SEM fractographs of (a) A1 and (b) A2 tensile specimens.

A1 and B1 consist of large ferrite grains, small ferrite grains and martensite. However, the ratio of each phase in A1 and B1 is different. Carbides are found in B1, but not in A1. The size of the large ferrite grains is in the range of ∼1–15 μm and the size of the small ferrite grains is smaller than ∼1 μm. It is noticeable that the distribution of small ferrite grains is in colonies in adjacent to the martensite. A2 and B2 are mainly composed of fine ferrite and carbide colonies. The sites of carbide colonies were initially pearlite regions. Pearlite was degenerated during rolling process and thus forming carbide colonies. A small amount of martensite was also found in A2.

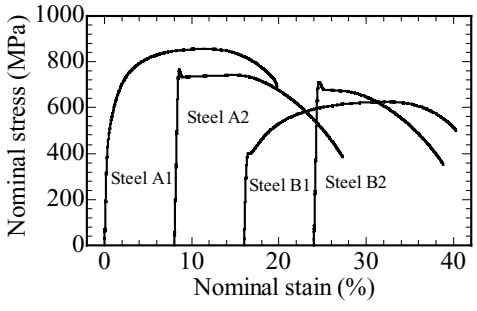

Figure 5 The stress-strain curves of A1, A2, B1 and B2.

3.2. Fracture mechanism

Tensile specimens of A1, A2, B1 and B2 break in ductile fracture mode at room temperature. The fracture surfaces of A1 and A2 are shown in Fig. 4. Separations are seen on the fracture surfaces of A2 and B2 while not found in A1 and B1. To examine the formation of voids in the four steels, broken tensile specimens were cut along the longitudinal center plane firstly, and then the longitudinal center planes were polished and etched with 3% nital. The SEM micrographs show that voids in A1 and B1 are mainly formed by the decohesion of martensite/matrix interfaces, and voids in A2 and B2 are mainly initiated from inclusions and carbides. Brittle fracture surfaces of A1 impact specimens at −80°C were observed by SEM. The SEM observation indicates that the cleavage crack initiates at martensite. Secondary cracks were found to be present on all of the surfaces of A1, A2, B1 and B2 at –80°C.

3.3. Tensile properties

Tensile results are summarized in Table II. The stress-strain curves of A1, A2, B1 and B2 are shown in Fig. 5. The curves of A1 and B1 show a striking contrast to those of A2 and B2. The former two steels have low yield ratio (YR) values (yield strength to tensile strength) while the YR of the latter two steels is extremely high (close to unity). The uniform elongations of the former two steels are significantly larger than those of the latter. The shapes of stress-strain curves are also different.

As shown in Fig. 3, A1 and B1 consist of large soft ferrite grains, relatively hard ferrite grain colony and hard martensite. Soft phase is easy to deform and hard phase, as a strengthening phase, could increase the strength of steel. The presence of soft and hard phases makes A1 and B1 have large tensile uniform elongation as well as high strength. By comparison, A2 and B2 are mainly composed of fine ferrite. Single ferrite phase steel has been verified to be detrimental to uniform elongation [6]. Therefore, low uniform elongation in A2 and B2 may be attributed to insufficient second or third soft phase. It can be concluded from the above results that A1 has the best combination of strength and uniform elongation among the four steels.

3.4. Dynamic fracture behavior

Fig. 6 gives the impact curves of A1, A2, B1 and B2. For A1 and B1, load increases gradually with time until maximum load point; and when exceeding the maximum load point, load decreases gradually with time. However, for A2 and B2, load rapidly and almost linearly increases with time until maximum load, and then rapidly decreases. Comparing with Fig. 5, it is found that the shape of impact curve is related to tensile stress vs. strain curve.

TABLE II Tensile properties

No.	$\sigma_s^{(MPa)}$	$\sigma_T^{(MPa)}$	U.EI (%)	YR
A1	476	855	11.4	0.56
A2	734	742	6.8	0.99
B1	401	625	16.2	0.64
B2	712	712	0.6	1

U.EI: uniform elongation; YR $= \sigma_s/\sigma_T$.

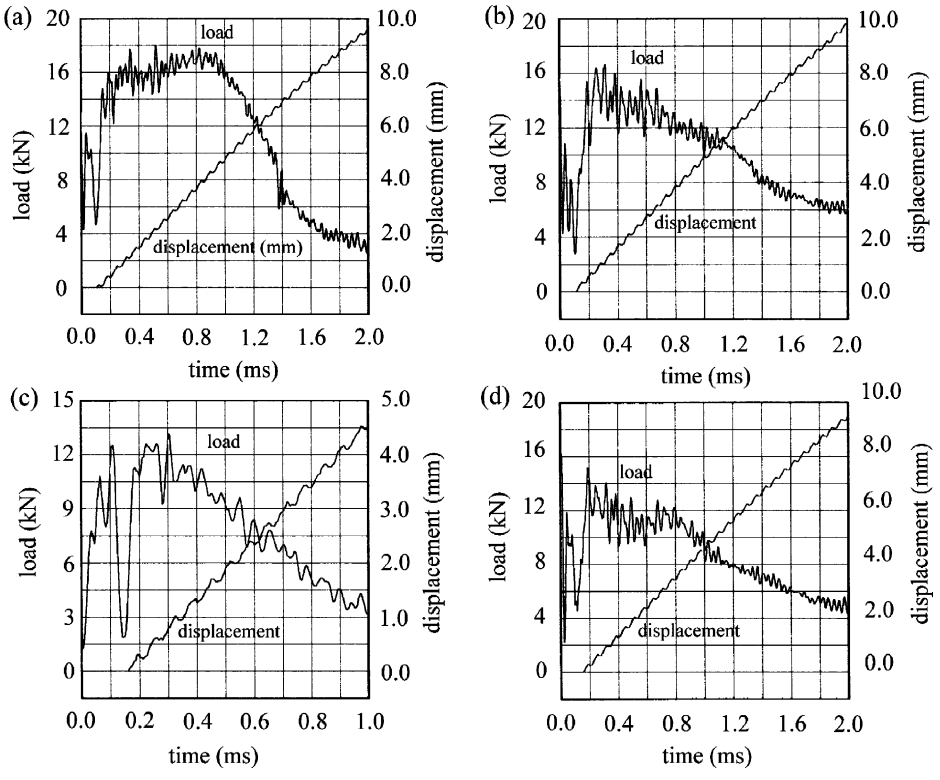

Figure 6 The dependence of load and displacement on time for (a) A1, at −60°C, (b) A2, at −80°C, (c) B1, at −40°C, and (d) B2, at −120°C.

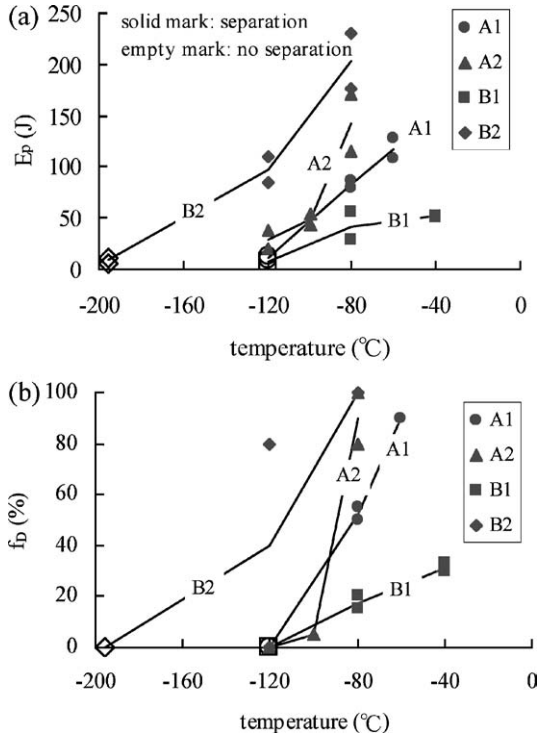

Figure 7 The dependence of (a) impact absorbed energy (E_p) and (b) ductile fracture ratio (f_D) on temperature for A1, A2, B1 and B2.

Impact absorbed energy (E_p) and ductile fracture ratio against temperature for A1, A2, B1 and B2 are plotted in Fig. 7. A2 has higher E_p than A1. B2 has the same tendency, too. It indicates that low temperature rolling is good for improving the impact behavior. B2 and B1 have the highest and smallest E_p, respectively, among the four steels. Solid and empty marks in Fig. 7, respectively, mean that separation takes place or not at those temperatures.

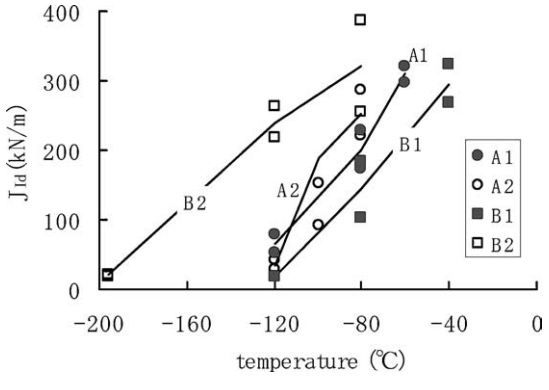

Figure 8 The dependence of J_{Id} on temperature for A1, A2, B1 and B2.

The dependence of J_{Id} on temperature for A1, A2, B1 and B2 is given in Fig. 8. The J_{Id} of the four steels decreases with temperature. It can also be seen from Fig. 8 that B1 and B2 have, respectively, the worst and best impact behavior among the four steels, which agrees with the results of impact absorbed energy (E_p). To investigate the correlation between E_p and J_{Id}, J_{Id} is plotted against E_p in Fig. 9. For a given steel, J_{Id} increases with E_p in spite of the scatter of data. Comparing the general varying tendency of J_{Id} with E_p for A1 and A2 in Fig. 9, the J_{Id} of A1 is found to be larger than that of A2 for the same E_p. B1 and B2 have the same tendency. This result indicates that the dynamic fracture toughness of different materials is not inevitably the same even if they have the same E_p, and that it is not sufficient to valuate the toughness of the ultra-fine grained steels only by E_p. It is suggested that the correlation between J_{Id} and E_p depends on the type of the tensile stress-strain curve.

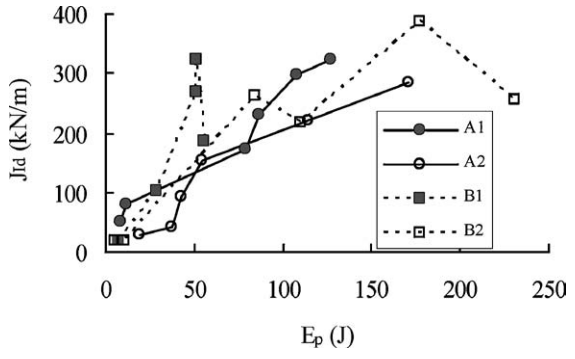

Figure 9 Correlation between J_{Id} and E_p for the ultra-fine grained steels.

4. Conclusions

1. Composite microstructures consisting of large ferrite grains, small ferrite grain colony and martensite are good for improving tensile uniform elongation. Such microstructures have a good combination of strength and ductility.

2. Impact curves of the ultra-fine grained steels are correlated with their tensile stress-strain curves.

3. Composite constituents consisting of large ferrite grains, small ferrite grain colony and martensite have not only high strength but also good toughness.

4. For the same E_p, the J_{Id} values of A1 and B1 are larger than those of A2 and B2, respectively. The toughness of the ultra fine grained steel is evaluated insufficiently only by E_p.

References

1. T. MAKI, *J. Jpn. Soc. Heat Treat.* **37**(1997) 5.
2. NATIONAL RESEARCH INSTITUTE FOR METALS, in Proc. of 98 Workshop of Structural Materials for 21st Century, Tsukuba, Japan, 1998.
3. NATIONAL RESEARCH INSTITUTE FOR METALS, in Proc. of 99 Workshop of Structural Materials for 21st Century, Tsukuba, Japan, 1999.
4. NATIONAL RESEARCH INSTITUTE FOR METALS, in Proc. of 2000 Workshop of Structural Materials for 21st Century, Tsukuba, Japan, 2000.
5. H. QIU, Y. KAWAGUCHI, C. SHIGA, M. ENOKI and T. KISHI, *Mater. Sci. Tchnol.* (in press).
6. N. MATSUKURA and S. NANBA, in Proc. of 1st Symposium on Super Metal, R&D Inst. of Met. and Composites for Future Industries (RIMCOF) and The Japan Res. and Development Center for Met. (JRCM), Tokyo, Japan, 1998, p. 229.

Received 22 October 2002
and accepted 11 February 2004